SPE 100611

Laboratory- and Field Prediction of Sulphate Scaling Damage

P. G. Bedrikovetsky, SPE, North Fluminense State University (LENEP/UENF); E. J. Mackay, SPE, Heriot-Watt University; R. P. Monteiro, North Fluminense State University (LENEP/UENF); P. M. Gladstone, Cefet-Campos/UNED Macaé; F. F. Rosário, SPE, Petrobras/CENPES

Abstract

$BaSO_4$ scaling can have a disastrous impact on production in waterflood projects with incompatible injected and formation waters. This is due to precipitation of barium sulphate from the mixture of both waters, the consequent permeability reduction resulting in loss of well productivity.

The system where sulphate scaling damage occurs is determined by two governing parameters: the kinetics coefficient characterising the velocity of chemical reaction and the formation damage coefficient reflecting permeability decrease due to salt precipitation.

Previous work has derived an analytical model-based method for determination the kinetics coefficient from laboratory corefloods during quasi-steady state commingled flow of injected and formation waters. The current study extends the method and derives formulae for calculation of the formation damage coefficient from pressure drop measurements during the coreflood.

The proposed method can be extended for axisymmetric flow around the well allowing calculation of both sulphate scaling damage coefficients from field data consisting of barium concentrations in the produced water and well productivity decline.

We analyse several laboratory test data and field data, and obtain values of the two sulphate scaling damage parameters. The values of kinetics and formation damage coefficients as obtained from either laboratory or field data vary in the same range intervals. These results validate the proposed mathematical model for sulphate scaling damage and the analytical model-based method “from lab to wells”.

Introduction

It has been long recognised that formation and well damage may be caused by incompatibility of injected and formation waters. Precipitation of salts results in permeability decline. Among the most significant of all scaling species are the sulphates, particularly barium and strontium sulphates[1-3].

Decision making on scale prevention and removal is based on prediction scale precipitation and damage is provided by mathematical modelling.

The mathematical models for sulphate scaling during waterflooding consist of mass balance equations for all species with the reaction rate sink terms[4–7]. Chemical reaction rate must obey law of acting masses[5,8,9] or another more complex kinetics law[9–14].

Several numerical[15,16] and analytical[4,17–19] models describing sulphate scaling under laboratory and field conditions are available in the literature.

Nevertheless, the problem of determining model coefficients from either laboratory or field data to use in sulphate scaling simulation is far from resolved. This

introduces significant uncertainty in prediction of scaling damage.

The design and results of barium sulphate quasi-steady state scaling tests have been presented in the literature[20–22]. The analytical model for quasi-steady state commingled flow of injected and formation waters in cores allows us to solve the inverse problems of determining scaling model parameters from laboratory test data[19].

The chemical reaction rate depends on the reaction rate coefficient. The reaction rate coefficient can be determined from effluent barium concentration using the analytical solution[19]. Treatment of laboratory data shows that the reaction rate is proportional to flow velocity, as it should be for reactive flows in porous media[8]. The proportionality coefficient is called the kinetics coefficient.

The kinetics coefficient depends on rock and fluid properties. It cannot be predicted theoretically for real reservoirs and fluids. Therefore, it must be determined from either laboratory or field data by solution of inverse problems.

The second important parameter determining permeability impairment during sulphate scaling is the formation damage coefficient, which shows how permeability decreases with solid deposition.

The analytical model for axisymmetric quasi-steady state commingled flow of injected and formation waters, describes the accumulation of sulphate salts near to production wells[23]. The model is based on the statement that the most significant scale formation damage during a waterflood occurs in the neighbourhood of production wells due to the intensive mixing and deposit accumulation[1] that occurs in this location. The model allows us to determine the kinetics coefficient of the barium sulphate reaction from barium concentration in produced water and to determine the formation damage coefficient from the productivity index history. The model is one-dimensional and does not account for inter layer diffusive transfer of reacting ions, which may impacts the well productivity damage. Nevertheless, the model can be used to evaluate orders of magnitude of kinetics and formation damage coefficients from production well data.

In the current work, we propose a method for calculation of the formation damage coefficient from the pressure drop in the core during quasi-steady state commingled flow of injected and formation waters. Treatment of several laboratory tests[20–22,24,25] reveals that the formation damage coefficient has the same order of magnitude as that obtained from deep bed filtration of colloid particles.

Several field cases were treated in order to estimate orders of magnitude for kinetics and formation damage coefficients, and it was found out that both coefficients have the same order of magnitude as those obtained from laboratory tests. It validates the proposed mathematical model with reaction rate coefficient proportional to flow velocity. It also validates the use of scaling damage coefficients “from lab to wells”.

Assumptions of the Barium Sulphate Scaling Model

We discuss formation damage due to barium sulphate precipitation (oilfield scaling) causing productivity impairment. Usually seawater is injected in offshore operations, and it contains SO_4^{2-} anions. If the formation water

contains Ba^{2+} cations, then mixing of injected and formation waters may cause $BaSO_4$ deposition (**Fig. 1a**).

$$Ba^{2+} + SO_4^{2-} \rightarrow BaSO_4 \downarrow \quad \text{.....(1)}$$

A schematic of injected and formation water mixing in a reservoir undergoing waterflooding is shown in **Fig. 1b**.

The main assumptions of the physical-mathematical model of barium sulphate scaling are:

- the chemical reaction between barium and sulphate ions is irreversible;
- this reaction is a second order chemical reaction obeying the mass action law;
- the chemical reaction rate coefficient is proportional to flow velocity;
- brine is incompressible;
- volume is conserved during brine mixing and salt precipitation;
- the dispersion coefficient is proportional to flow velocity;
- the rate coefficient is independent of the precipitant concentration;
- the permeability decline versus precipitant concentration takes a hyperbolic form.

Irreversibility of chemical reaction between barium and sulphate ions can be assumed because of the low solubility of barium sulphate salt in water[12–14].

The mathematical model for flow of injected and formation waters in porous media includes mass balance equations for barium cations, for sulphate anions and for salt molecules, eq. A-1. The salt deposition rate is given by the law of mass action[4,5,8–11,17,18], eq. A-2. The modified Darcy's law eq. A-3 contains the formation damage coefficient β that describes permeability loss due to salt deposition.

The unknowns in the closed system of four equations, eq. A-4, are three concentrations and pressure.

The assumption that the reaction rate coefficient K_a is independent of the precipitated salt concentration σ, which is valid for small deposited concentrations, results in separation of the first and second equations A-4 from the rest of the system.

Proportionality between the dispersion coefficient and flow velocity was reported in numerous studies[1,7]:

$$D = \alpha_D U \quad \text{.....(2)}$$

Here α_D is a linear size of the core micro heterogeneity.

Proportionality between the reaction rate coefficient K_a and flow velocity was observed generally for reactive flows in porous media[8] and specifically for the sulphate scaling reactions[19,22]:

$$K_a = \lambda U \quad \text{.....(3)}$$

The proportionality coefficient λ is called the kinetics coefficient. It is equal to the reciprocal of the average distance that the mole of the ion travels in the rock before being consumed by the chemical reaction.

In dimensionless co-ordinates (see eq. A-6), the system of governing equations takes the form in the eq. A-7.

$$\begin{cases} \dfrac{\partial C}{\partial t_D} + \dfrac{\partial C}{\partial x_D} = \varepsilon_D \dfrac{\partial^2 C}{\partial x_D^2} - \varepsilon_k C Y \\ \dfrac{\partial Y}{\partial t_D} + \dfrac{\partial Y}{\partial x_D} = \varepsilon_D \dfrac{\partial^2 Y}{\partial x_D^2} - \varepsilon_k \alpha C Y \end{cases} \quad \text{.....(4)}$$

where α is a ratio between the initial concentrations of Ba^{2+} in formation water and of SO_4^{2-} in injected seawater.

The system of eq. 4 contains the dimensionless chemical kinetics number ε_k, and the diffusive number ε_D, which is the inverse of the Peclet number[7,8].

$$\varepsilon_k = \frac{K_a c^0_{SO_4} L}{U} = \lambda c^0_{SO_4} L \ , \ \varepsilon_D = \frac{D}{LU} = \frac{\alpha_D}{L} \quad \text{.....(5)}$$

The inlet boundary conditions, eq. A-8, correspond to fixed fluxes of sulphate and of barium via the inlet cross-section. The assumption of negligible diffusion simplifies the inlet conditions, as seen in eq. A-9.

For the range of velocities occurring in petroleum reservoirs, advective mass transfer greatly exceeds the diffusive flux. So, if the species particle has already left the core, it would not diffuse back. The corresponding outlet boundary condition is given by eq. A-10[7].

For quasi-steady state tests, the system of equations 4 is reduced to a system of ordinary differential equations B-2. The boundary conditions, eqs. B-3 and B-4, correspond to simultaneous injection of sea and formation waters with fixed barium and sulphate concentrations.

For the case where sulphate and barium concentrations have the same order of magnitude (α~1), Runge-Kutta method was used to solve the ordinary differential eq. B-12.

For the case where the sulphate concentration in seawater greatly exceeds the barium concentration in formation water (α<<1) the steady state concentration profiles are described by explicit equations C-2 to C-5.

Methodology of Laboratory Tests

The objective of the laboratory study is the determination of the kinetics and formation damage coefficients for rock flow conditions.

The experimental setup[19,22] consists of a core holder with confinement, two pumps, and pressure transducers. The core holder has two independent inlet tubes allowing for simultaneous injection of two different reagents. The set-up schema is given in **Fig. 2**. Similar set-ups were used in other laboratory studies[20,21,24,25].

The flood sequence that allows determination of the two sulphate scaling damage parameters is:

1. Diffusion tests:

1.1. Saturation of core with synthetic formation water;

1.2. Injection of synthetic seawater without SO_4^{2-} anions at some given velocity;

1.3. Injection of synthetic formation water at another given velocity;

1.4. Further alternate injections of synthetic formation and seawaters at different velocities.

2. Transient tests:

2.1. Saturation of core with synthetic formation water at the final stage of the diffusive tests;

2.2. Injection of synthetic seawater at some given velocity;

2.3. Injection of synthetic formation water at another given velocity.

3. Quasi steady state tests (**Fig. 3**):

3.1. Simultaneous injection of formation and seawaters at some given velocity;

3.2. Further simultaneous injections of formation and seawaters at different velocities.

Diffusivity tests. The objective of the diffusivity tests is to determine of core rock dispersivity α_D.

Fig. 4 shows the dependencies "dispersion versus velocity" for two cores[19,22]. The linear dependence $D(U) = \alpha_D U$ allows good adjustment of the data.

For two cores, the α_D values found are 0.018 m and 0.011 m, which is quite reasonable for 0.1 m long real reservoir cores.

It is important to emphasise that tracer tests must accompany sulphate scaling tests: otherwise the dispersivity α_D becomes an additional unknown parameter. The number of unknowns together with kinetics and formation damage coefficients would become three. Nevertheless, the number of measured values is two (effluent concentration and pressure drop on the core). Therefore, the sulphate scaling system could not be fully characterised.

For example, the tracer test data for sulphate scaling tests[21,24,25] are not available. Therefore, the kinetics and formation damage coefficients have been determined assuming some typical α_D values (**Tables 1,2 and 4**).

Steady state tests. The objective of the quasi-steady state tests is the determination of kinetics and formation damage coefficients from outlet concentration and pressure drop data for the core.

The system of governing equations B-2 as applied for steady state flows may be reduced to a single second order ordinary differential equation (ODE), eq. B-12.

The boundary conditions for the second order ODE correspond to given reagent concentrations at the core inlet eq. B-3 and to the absence of diffusion at the core outlet eq. A-10. For the case $\alpha<<1$ the equation B-12 is subject to boundary conditions eqs. B-3 and A-10 allows for the explicit asymptotic solution. Zero order approximation is given by equations C-3 to C-5. First and second order approximations are expressed by explicit but rather cumbersome formulae; see eqs. C-7 to C-10.

The expansion, eq. C-1, converged rather fast. Even for α=1 first order approximation gives a good match with numerical solution (**Fig. 5**). The second order approximation almost coincides with the numerical solution.

Fig. 6 presents relative error for zero-, first- and second-order approximations if compared with numerical solution. Calculations have been performed for ε_k= 9.37. Plots allow determining relative error for different order approximations. For example, for α= 0.2, error for second order approximation is equal to 0.02; first order approximation provides with the error 0.11, and zero order approximation gives 0.45.

The analytical model-based calculations have been performed in the current paper using the second order approximation.

The first objective of the study was to determine the kinetics number ε_k from the barium steady state effluent concentration $C(x_D= 1)$**.** Thus, the value $C(x_D= 1)$**,** as obtained from laboratory coreflood data, was fitted to the analytical

solution at the effluent in eq. C-6 by adjusting the kinetics number ε_k.

Figs. 7a and 7b show the reaction rate coefficient K_a versus velocity for two cores[19,22].

Values of λ for two cores are 3003 and 3951 $(M*m)^{-1}$ (Figs. 7a and 7b).

The proportionality between the reaction rate number and flow velocity, eq. 3, takes place for catalytic chemical reactions for low flow velocities, where the reaction is controlled by diffusion[8].

The dependency of reaction rate coefficient on flow velocity must be used in reservoir simulators[16] when performing scaling reaction calculations.

The second objective of the steady state tests is the calculation of the formation damage coefficient β.

If kinetics coefficient λ and dispersivity α_D are known, the impedance growth allows us to determine the formation damage coefficient. The impedance slope *m* is calculated from pressure drop data using first eq. D-7. From the second eq. D-7 follows the expression for the formation damage coefficient. The right hand side of eq. D-7 depends on the kinetic number that was obtained from the outlet concentration data. The integral is calculated either analytically or numerically together with the solution of the concentration problem described by eqs. B-2, B-3 and A-10. The kinetics number is calculated by eq. 5 using the previously obtained kinetics coefficient, λ.

Now let us describe the results of the treatment of laboratory data presented in the literature[19–22,24,25].

Outlet barium concentration and pressure drop were measured in coreflood studies[21,24,25]. Unfortunately, tracer tests have not been performed. Therefore, the results for two sulphate scaling damage parameters are presented in Tables 1,2 and 4 as functions of rock dispersivity.

Tables 1 and 2 present treatment results from laboratory data[21,24]. The brine sample compositions and rock properties can be found in the original paper[21].

Table 1 corresponds to a temperature of 20°C, **Table 2** corresponds to a temperature of 70°C.

We took a reference value for dispersivity α_D= 0.01 m which is quite typical for homogeneous sandpacks, and performed a sensitivity study with respect to dispersivity. The range interval for the kinetics coefficient for α_D= 0.01 m is 250 to 20000 $(M*m)^{-1}$. Variation of dispersivity does not change the lower bound; it doubles the upper bound–40000 $(M*m)^{-1}$.

The formation damage coefficient varies in the range 10 to 100. The formation damage coefficient as calculated from deep bed filtration tests varies in a wider interval 10 to 2000[26,27].

Another set of laboratory tests is presented in[25]. The dispersivity has not been measured; so we fixed three values for dispersivity coefficient that are typical for high permeability homogeneous sandpacks: α_D= 0.005, 0.01 and 0.03 m. **Table 3** shows compositions of sample brines used in the tests. **Table 4** presents the obtained values for two scaling damage parameters.

For dispersivity value α_D= 0.01 m, kinetics coefficient varies from 40000 to 120000. Variation of dispersivity from

α_D= 0.005 m to α_D= 0.03 m almost does not change this interval.

The derived kinetics coefficient values are one order of magnitude higher than those obtained in other tests due to the very low effluent barium concentrations. The author[25] also noticed that effluent barium concentrations are very low and attributed it to a delay in analysis of the produced samples.

Nevertheless, the formation damage coefficient varies in the usual interval 30 to 3000.

In the work[20], simultaneous injection of formation and seawaters has been carried out. The sandpack with permeability k= 30 mD and porosity ϕ= 0.37 was flooded simultaneously by seawater with sulphate concentration c_{SO4}^0= 0.031 M and by formation water with barium concentration c_{Ba}^0= 0.0018 M. Barium concentrations were measured at the core effluent. The barium concentration reached at the steady state c_{Ba} (x_D= 1)= 3.5 ppm after 1 p.v.i.

The results are placed in **Table 5**. The values obtained for the kinetics coefficient lay in the interval covered by the above-mentioned tests.

During coreflooding by reacting seawater and formation water in work[19,22], tracer outlet concentrations were monitored. Therefore, the derived kinetics constant data are more reliable. Table 5 presents interval 3000 to 4000. The pressure drop did not increase significantly during the short flood period; therefore it was not enough information to make a reliable calculation of the formation damage coefficient.

The scaling damage parameters as obtained from the four above-mentioned sets of laboratory tests are presented in table 5. Depending on the reservoir temperature, the brine ionic strength and rock permeability, the kinetics coefficient varies from 200 to 130000 $(M*m)^{-1}$. The formation damage coefficient varies from 30 to 3000.

Probabilistic distributions of the kinetics coefficient λ and the formation damage coefficient β as obtained from laboratory corefloods are presented in **Figs. 8a and 8b** respectively. Large interval for λ variation is caused by unknown dispersion coefficient in majority of tests; the results include λ-values as calculated for various dispersivities (Tables 1,2 and 4). The formation damage coefficient β varies from 9 to 3000; the variation interval almost coincides with that obtained for deep bed filtration of particle suspensions in porous media[26,27].

Transient precipitation tests. Transient precipitation tests were performed in order to verify the unsteady state model, eq. 4, in general, and specifically the dependence of reaction rate coefficient versus velocity, as obtained from the quasi steady state tests.

The verification of the model 4 has been performed by comparison between the laboratory test data and the simulation results using the data obtained from the steady state tests. The laboratory and modelling data are in a reasonable agreement[19,22].

Determination of Kinetics and Formation Damage Coefficients from Field Data

The method for calculation of kinetics and formation damage coefficients from barium concentration in produced water and productivity index history is also based on analytical solution

of reactive flow equation around production wells[23]. The analytical axisymmetric model and corresponding inverse problems are similar to those for corefloods presented in previous sections of the current paper.

The main model assumptions are based on the fact that salt accumulation during waterflooding occurs mainly near to production wells[1].

The main assumptions of the model are steady state flow in the neighbourhood of the production well, second order chemical reaction between barium and sulphate ions, the irreversibility of the reaction, and proportionality of the relationships "dispersion versus velocity" and "chemical rate coefficient versus velocity". These assumptions correspond to near well flow conditions.

The model is one-dimensional, i.e. vertical diffusive flux between layers with different permeability is neglected. Also, it is assumed that reaction is occurring only near to the production wells. This assumption limits the model applicability.

Nevertheless, while not being able to determine the exact values for scaling damage parameters from well data, the model does provide us with their order of magnitude.

Figs. 9 and 10 present data for a highly permeable, low heterogeneity, large net pay offshore sandstone field X (Campos Basin, Brazil)[28,29]. Production well X1 is completed with a gravel pack where intensive barium sulphate accumulation takes place due to high flow velocity and, concequently, high dispersion. It confirms the model assumption that significant chemical reaction and deposition occurs only in the well vicinity. Works[28,29] state that for the case of the two producers from field X, the major precipitant accumulation occurs in the gravel pack. It justifies application of the analytical axi symmetric reactive flow model[23].

The best fit of the curve "barium concentration in produced water versus seawater fraction in produced water" using least square method was achieved for λ=117234 $(M*m)^{-1}$.

The formation damage coefficient was obtained by adjustment of the productivity index curve. Three measurements of productivity index were performed shortly after one another, so effectively just one PI value is available. Linear approximation results in the value for formation damage coefficient β= 0.5. We attribute the small value of the formation damage coefficient to the fact that precipitation occurs mostly in the gravel pack for the well discussed. The porous medium in the gravel pack is highly permeable and homogeneous, so some permeability decline occurs only after significant deposition.

Fig. 11 presents the barium concentration in the produced water for another well with gravel pack from the field X. The obtained kinetics coefficient is lower than that obtained from another well (**Table 6**).

The data on barium concentration in the producing water and on productivity index decline were treated for field Namorado (Campos Basin, Brazil)[30] and for five North Sea fields[31].

Probabilistic distributions of kinetics constant λ and formation damage coefficient β as obtained from well data are presented in **Figs. 12a and 12b** respectively; corresponding data are given in **Table 7**. Large interval for λ variation is

caused by unknown dispersion coefficient in majority of tests; the results include λ-values as calculated for various dispersivities. The formation damage coefficient β varies from 0.5 to 2000; the variation interval almost coincides with that obtained for deep bed filtration of particle suspensions in porous media[26,27]. Low values for formation damage coefficient for field X (Table 7) are explained by the fact that scaling happens mainly in gravel packs of the wells[28,29].

Discussions

The main result of the current paper is that the kinetics coefficient as obtained from laboratory and field data varies in the same range interval. The same was observed for the formation damage coefficient.

The kinetics coefficient varies from 50 to 100000 depending on brine ionic strength and temperature for either coreflood or well data. The interval covers all cases between no reaction and intensive barium sulphate deposition.

The interval is huge, and it is the same for either coreflood or well cases. It supports the statement that the physical processes occurring in cores and near production wells and the resulting permeability decrease, are the same.

It is well known that the permeability as obtained from well test and from the same field cores can differ by one order of magnitude. Nevertheless, the permeability varies 10^4 times from field to field, so comparison between core and well test data may provide important information about the reservoir. The same applies to sulphate scaling damage parameters. Unfortunately, the data on productivity index decline for scaled-up wells and on permeability impairment during scaling in the core taken from the same well are not available in the literature.

Under the circumstances, we conclude that both sulphate scaling damage parameters as obtained from corefloods, vary in the same intervals as those obtained from well histories.

Conclusions

Analytical-model-based treatment of laboratory and field data on sulphate scaling formation damage allows concluding as follows:

1. An analytical model for quasi steady state reactive flow of injected and formation waters allows calculation of formation damage coefficient from the history of pressure drop on the core during coreflood test along with the calculation of the kinetics constant from the barium effluent concentration.
2. The kinetics and formation damage coefficients, as obtained from corefloods, vary in the same range intervals as those calculated from well data.
3. A database for kinetics and formation damage coefficients obtained from twenty-two laboratory tests and nineteen wells from seven fields must be used in reservoir simulation of waterflooding that includes sulphate scaling calculations.

Acknowledgement

The authors thank Dr. Maria Carmen Bezerra, Dr. Antonio Luis S. de Souza, Alexandre G. Sequeira, Dr. Farid Shecaira and Maylton Silva (Petrobras), Prof. Themis Carageorgos

(UENF-Lenep), Dr. Oleg Dinariev and Prof. A. D. Polianin (Russian Academy of Sciences) for fruitful discussions.

Many thanks are due to Eng. Sergio Daher (Petrobras) for several useful discussions and for proof reading the paper before its publication.

The authors thank Petrobras for permission to publish the paper.

Nomenclature

c_{Ba}= Ba^{2+} molar concentration in aqueous solution, nºmol/L^3, gmol/liter

c_{SO4}= SO_4^{2-} molar concentration in aqueous solution, nºmol/L^3, gmol/L

C = dimensionless Ba^{2+} concentration

D = dispersion coefficient, L^2/t, m^2/s

h = thickness, L, m

PI= productivity index, L^4t/m, $m^3/(s{\cdot}Pa)$

J = dimensionless impedance

k_0 = initial permeability, L^2, mD

K_a = chemical reaction rate constant, $(M{*}s)^{-1}$ (2^{nd} order reaction)

m = slope of the impedance straight line

M = molar unit for concentration equals gmol/L (same as kgmol/m^3)

M_{BaSO4} = molecular weight for Barium Sulphate equals 0.23339 Kg/mol

p = Pressure, m/Lt^2, Pa

p_D = dimensionless pressure

Q = total rate, L^3/t, m^3/s

R_c = contour radius, L, m

r_w = well radius, L, m

S = dimensionless $BaSO_4$ concentration

t = time, t, s

t_D = dimensionless time

U = flow velocity, L/t, m/s

V = concentration difference

x = linear co-ordinate, L, m

x_D = dimensionless coordinate

Y = dimensionless SO_4 concentration

Greek letters

α = ratio between injected concentrations of Ba^{2+} and SO_4^{2-}

α_D= dispersion coefficient, L, m

β = formation damage coefficient

ε_D = dimensionless diffusive (Schmidt) number

ε_k = dimensionless chemical kinetics number

ϕ = Porosity

λ = kinetic coefficient, $(M{*}m)^{-1}$ (2^{nd} order reaction)

μ = viscosity, m/Lt, kg/(m·s)

ρ_{BaSO4}= density of the Barite, 4193.9 Kg/m^3

σ = $BaSO_4$ molar concentration in solid deposit

References

1. Sorbie, K.S. and Mackay, E.J.: "Mixing of Injected, Connate and Aquifer Brines in Waterflooding and its Relevance to Oilfield Scaling," *Journal Petroleum Science Engineering* (2000) **27**, 85–106.
2. Rosario, F.F. and Bezerra, M.C.: "Scale Potential of a Deep Water Field – Water Characterisation and Scaling

Assessment," paper SPE 68332 presented at the 2001 SPE Third International Symposium on Oilfield Scaling, Aberdeen, UK, 30–31 January.

3. Oddo, J.E. and Tomson, M.B.: "Why Scale Forms and How to Predict It," *SPEPF* (February 1994) 47–54.
4. Philips, O.M.: *Flow and Reactions in Porous Media,* Cambridge University Press (1991).
5. Bedrikovetsky, P.G.: *Mathematical Theory of Oil and Gas Recovery,* Kluwer Academic Publishers, London/Boston (1994).
6. Green, D.W. and Willhite, G.P.: *Enhanced Oil Recovery,* Textbook Series, SPE, (1998).
7. Nikolaevskii, V.N.: *Mechanics of Porous and Fractured Media,* World Scientific Publishing Co., Singapure (1990).
8. Fogler, S.: *Chemical Reactions Engineering,* Prentice Hall, New York City, (1998).
9. Bethke, C.: *Geochemical Reaction Modelling,* Oxford University Press, (1996) 397.
10. Stumm, W.: *Chemistry of Solid-Water Interface,* John Wiley and Sons, New York City, (1992) 428.
11. Nielsen, A.E.: "The Kinetics of Crystal Growth in Barium Sulphate Precipitation II – Temperature Dependence and Mechanism," *Acta Chemical Scandinavica* (1959) 13, 784–802.
12. Christy, A.G. and Putnis, A.: "The Kinetics of Barite Dissolution and Precipitation in Water and Sodium Chlorite Brines at 44–850°C," *Geochimica et Cosmochimica Acta* (1992) 57, 2161-2168.
13. Nancollas, G. and Liu, T.: "Crystal Growth and Dissolution of Barium Sulphate", paper SPE 5300 presented at the 1975 SPE/AIME Oilfield Chemistry Symposium, Dallas, January.
14. Atkinson, G. and Raju, K.: "The Thermodynamics of Scale Precipitation," paper SPE 21021 presented at the 1991 SPE Simposium on Oilfield Chemistry, Anaheim, Ca, 21–23 February.
15. Rocha, A. *et al.*: "Numerical Modelling of Salt Precipitation during Produced Water Reinjection," paper SPE 68336 presented at 2001 SPE Third International Symposium on Oilfield Scale, Aberdeen, UK, 30–31 January.
16. Delshad M. and Pope, G.A.: "Effect of Dispersion on Transport and Precipitation of Barium and Suphate in Oil Reservoir," paper SPE 80253 presented at the 2003 SPE International Symposium on Oilfield Chemistry, Houston, Texas, USA, 5–7 February.
17. Woods, A.W. and Parker, G.: "Barium Sulphate Precipitation in Porous Rock Through Dispersive Mixing," paper SPE 80401 presented at the 2003 SPE 5th International Symposium on Oilfield Scale, Aberdeen, UK, 29–30 January.
18. Araque-Martinez, A. and Lake, L.W.: "A Simplified Approach to Geochemical Modelling and its Effect on Well Impairment," paper SPE 56678 presented at the 1999 SPE Annual Technical Conference and Exhibition, Houston, Texas, 3–6 October.
19. Bedrikovetsky, P.G. *et al.*: "Barium Sulphate Oilfield Scaling: Mathematical and Laboratory Modelling," paper SPE 87457 presented at the 2004 SPE 6th International Symposium on Oilfield Scaling, Aberdeen, UK, 25–26 May.
20. Wat, R.M.S., Sorbie, K.S. and Todd, A.C.: "Kinetics of $BaSO_4$ Crystal Growth and Effect in Formation Damage," paper SPE 23814 presented at the 1992 SPE International

Symposium on Formation Damage Control, Lafayette, Louisiana, 26–27 February.

21. Todd, A.C. and Yuan, M.D.: "Barium and Strontium Sulphate Solid-Solution Scale Formation at Elevated Temperatures," *SPEPE* (February 1992) 85–92.
22. Lopes Jr., R.P., "Barium Sulphate Kinetics of Precipitation in Porous Media: Mathematical and Laboratory Modelling," in Portuguese, MS Thesis, North Fluminense State University-Lenep/UENF, Macaé, RJ, Brazil (2002).
23. Bedrikovetsky, P.G. *et al.*: "Oilfield Scaling – Part II: Productivity Index Theory," paper SPE 81128 presented at the 2003 SPE Latin American and Caribbean Petroleum Engineering Conference, Port-of-Spain, Trinidad, West Indies, 27–30 April.
24. Yuan, M.: "Prediction of Sulphate Scaling Tendency and Investigation of Barium and Strontium Sulphate Solid Solution Scale Formation," PhD dissertation, Heriot-Watt University, Scotland (1989).
25. Goulding, P. S.: "Formation Damage Arising from Barium Sulphate Scale Precipitation," PhD dissertation, Heriot-Watt University, Scotland (1987).
26. Bedrikovetsky P.G. *et al.*: "Characterization of Deep Bed Filtration System from Laboratory Pressure Drop Measurements," *Journal of Petroleum Science and Engineering* (2001) 64, No. 3, 167–177.
27. Bedrikovetsky, P.G. *et al.*: "Characterization of Deep Bed Filtration from Pressure Measurements," *SPEPF* (2003) No 3, 119–128.
28. Daher, J.S.: "Avaliação de Incrustação de Sais Inorgânicos em Reservatórios Inconsolidados Através da Simulação Numérica," in Portuguese, MS Thesis, North Fluminense State University-Lenep/UENF, Macaé, RJ, Brazil (2003).
29. Daher, J.S. *et al.*: "Evaluation of Inorganic Scale Deposition in Unconsolidated Reservoir by Numerical Simulation," paper SPE 95107 presented at the 2005 SPE 7th International Symposium on Oilfield Scale, Aberdeen, UK, 11–12 May.

Appendix A. Governing Equations

The mass balance for ions Ba^{2+}, SO_4^{2-} and for $BaSO_4$ molecules is[4,17–19]:

$$\begin{cases} \phi\dfrac{\partial c_{Ba}}{\partial t}+U\nabla c_{Ba}=\nabla\left(D\nabla c_{Ba}\right)-q \\ \phi\dfrac{\partial c_{SO_4}}{\partial t}+U\nabla c_{SO_4}=\nabla\left(D\nabla c_{SO_4}\right)-q \\ \phi\dfrac{\rho_{BaSO_4}}{M_{BaSO_4}}\dfrac{\partial\sigma}{\partial t}=q \end{cases} \quad \text{.....(A-1)}$$

The law of mass action is assumed for the chemical reaction (salt deposition) rate[8]

$$q=K_a c_{Ba} c_{SO_4} \quad \text{.....(A-2)}$$

The modified Darcy's law includes the permeability damage due to salt precipitation:

$$U=-\frac{k}{\mu\left(1+\beta\sigma\right)}\nabla p \quad \text{.....(A-3)}$$

The system of five equations A-1 to A-3 is closed. The unknowns are three concentrations c_{Ba}, c_{SO4}, σ, and pressure p.

The linear problem describes one-dimensional flow during laboratory coreflooding:

$$\begin{cases} \phi\dfrac{\partial c_{Ba}}{\partial t}+U\dfrac{\partial c_{Ba}}{\partial x}=D\dfrac{\partial^2 c_{Ba}}{\partial x^2}-K_a c_{Ba}c_{SO_4} \\ \phi\dfrac{\partial c_{SO_4}}{\partial t}+U\dfrac{\partial c_{SO_4}}{\partial x}=D\dfrac{\partial^2 c_{SO_4}}{\partial x^2}-K_a c_{Ba}c_{SO_4} \\ \phi\dfrac{\rho_{BaSO_4}}{M_{BaSO_4}}\dfrac{\partial\sigma}{\partial t}=K_a c_{Ba}c_{SO_4} \\ U=-\dfrac{k}{\mu(1+\beta\sigma)}\dfrac{\partial p}{\partial x} \end{cases} \quad \text{……..……(A-4)}$$

It is assumed that the diffusion coefficients for Ba^{2+} and SO_4^{2-} ions are equal and proportional to flow velocity:

$$D_{Ba}\cong D_{SO_4}\cong D=\alpha_D U \quad \text{……...(A-5)}$$

Let us introduce the following dimensionless parameters:

$$C=\frac{c_{Ba}}{c_{Ba}^0},\ Y=\frac{c_{SO_4}}{c_{SO_4}^0},\ x_D=\frac{x}{L}$$

$$t_D=\frac{Ut}{\phi L},\ \alpha=\frac{c_{Ba}^0}{c_{SO_4}^0},\ S=\frac{\rho_{BaSO_4}}{M_{BaSO_4}}\frac{\sigma}{c_{Ba}^0} \quad \text{……...(A-6)}$$

$$\varepsilon_D=\frac{D}{LU}=\frac{\alpha_D}{L}\quad \varepsilon_k=\frac{K_a L c_{SO_4}^0}{U}$$

First two equations A-4 take the form:

$$\begin{cases} \dfrac{\partial C}{\partial t_D}+\dfrac{\partial C}{\partial x_D}=\varepsilon_D\dfrac{\partial^2 C}{\partial x_D^{\,2}}-\varepsilon_k CY \\ \dfrac{\partial Y}{\partial t_D}+\dfrac{\partial Y}{\partial x_D}=\varepsilon_D\dfrac{\partial^2 Y}{\partial x_D^{\,2}}-\varepsilon_k \alpha CY \end{cases} \quad \text{……(A-7)}$$

Simultaneous injection of seawater containing SO_4^{2-} anions with Ba^{2+}-rich formation water corresponds to the inlet boundary conditions where fluxes are fixed for both species[7]:

$$x_D=0\ :\ C-\varepsilon_D\frac{\partial C}{\partial x_D}=1\ ,\ Y-\varepsilon_D\frac{\partial Y}{\partial x_D}=1 \quad \text{……(A-8)}$$

Neglecting the diffusive term simplifies the inlet boundary condition in eq. A-8:

$$x_D=0\ :\ C=1\ ,\ Y=1 \quad \text{……...(A-9)}$$

The assumption that an ion does not diffuse back into the core after leaving the outlet together with the carrier water, results in the Brenner's boundary condition[7]:

$$x_D=1:\frac{dC}{dx_D}=\frac{dY}{dx_D}=0 \quad \text{……..(A-10)}$$

Appendix B. Steady State Linear Flow

Let us consider steady state linear flow in a core:

$$\frac{\partial C}{\partial t_D}=\frac{\partial Y}{\partial t_D}=0 \quad \text{……(B-1)}$$

Substituting eq. B-1 into the first two equations A-7, obtain the following ordinary differential equations:

$$\begin{cases} \dfrac{dC}{dx_D}=\varepsilon_D\dfrac{d^2C}{dx_D^{\,2}}-\varepsilon_k CY \\ \dfrac{1}{\alpha}\dfrac{dY}{dx_D}=\dfrac{\varepsilon_D}{\alpha}\dfrac{d^2Y}{dx_D^{\,2}}-\varepsilon_k CY \end{cases} \quad \text{……..(B-2)}$$

Advection-diffusion fluxes of both components are fixed at the core inlet[7]:

$$x_D=0\ :\ C-\varepsilon_D\frac{dC}{dx_D}=1 \quad \text{……..(B-3)}$$

$$x_D=0\ :\ Y-\varepsilon_D\frac{dY}{dx_D}=1 \quad \text{……..(B-4)}$$

As a consequence of neglecting diffusion at the core inlet, the injected concentrations for both reagents are fixed at x_D=0:

$$x_D=0\ :\ C=Y=1 \quad \text{……..(B-5)}$$

If the particle has already left the core, it would not diffuse back. The corresponding outlet boundary conditions are given by eq. A-10.

So, the steady state chemical distribution along the core during the flow is described by a boundary problem, eqs. B-3

and B-4 for the system of two ordinary differential equations B-2.

Let us introduce the following linear combination of two concentrations:

$$V(x_D) = C(x_D) - \frac{Y(x_D)}{\alpha} \quad \text{.....(B-6)}$$

The subtraction of the second equation B-2 from the first one results in the following equation for the function $V(x_D)$:

$$\frac{dV}{dx_D} = \varepsilon_D \frac{d^2V}{dx_D^2} \quad \text{.....(B-7)}$$

The following inlet boundary condition for $V(x_D)$ follows from eq. B-3:

$$x_D = 0 \ : V = 1 - \frac{1}{\alpha} \quad \text{.....(B-8)}$$

The outlet boundary condition for $V(x_D)$ follows from eq. A-10:

$$x_D = 1 \ : \ \frac{dV}{dx_D} = 0 \quad \text{.....(B-9)}$$

Integrating both parts of eq. B-7 accounting for boundary conditions in eqs. B-8 and B-9 results in the solution:

$$V(x_D) = 1 - \frac{1}{\alpha} \quad \text{.....(B-10)}$$

So, the concentration difference in the eq. B-6 is constant along the core during the steady state flow.

Expressing the sulphate concentration $Y(x_D)$ from eq. B-10.

$$Y(x_D) = 1 + \alpha\left[C(x_D) - 1\right] \quad \text{.....(B-11)}$$

and substituting it into the first equation B-2, we obtain an ordinary differential equation for $C(x_D)$:

$$\varepsilon_D \frac{d^2C}{dx_D^2} = \frac{dC}{dx_D} + \varepsilon_k C\left[1 + \alpha\left(C - 1\right)\right] \quad \text{.....(B-12)}$$

Appendix C. Asymptotic Expansions Solutions for Concentration Profiles

Usually the sulphate concentration in seawater significantly exceeds the barium concentration in formation water. In this case, parameter α is negligibly small, $\alpha << 1$, (see eq. A-6).

Let us find asymptotic solution for the steady state flow problem described by eqs. B-12, A-10 and B-3 for small parameter α:

$$C(x_D) = C_0(x_D) + \alpha C_1(x_D) + \frac{\alpha^2}{2} C_2(x_D) \quad \text{.....(C-1)}$$

The term $[C(x_D)-1]$ varies from minus unity to zero, so the second term in brackets on the right hand side of eq. B-12 can be neglected comparing it with unity. Substituting expansion eq. C-1 into eq. B-12 obtain a linear second order ordinary differential equation for zero order approximation:

$$\varepsilon_D \frac{d^2C_0}{dx_D^2} = \frac{dC}{dx_D} + \varepsilon_k C \quad \text{.....(C-2)}$$

The boundary problem described by eqs. B-3 and A-10 for equation C-2 allows for exact solution:

$$C(x_D) = c_1 e^{\Gamma_1 x_D} + c_2 e^{\Gamma_2 x_D}$$
$$\Gamma_1 = \frac{1}{2\varepsilon_D} + \sqrt{\frac{1 + 4\varepsilon_D\varepsilon_k}{4\varepsilon_D^2}} \quad \text{.....(C-3)}$$
$$\Gamma_2 = \frac{1}{2\varepsilon_D} - \sqrt{\frac{1 + 4\varepsilon_D\varepsilon_k}{4\varepsilon_D^2}}$$

Two constants in eq. C-3 are found from boundary conditions, eqs. B-3 and A-10:

$$c_1 = \frac{-\Gamma_2 e^{(\Gamma_2 - \Gamma_1)}}{\Gamma_1 - \Gamma_2 e^{(\Gamma_2 - \Gamma_1)} + \varepsilon_D\Gamma_2\Gamma_1 e^{(\Gamma_2 - \Gamma_1)} - \varepsilon_D\Gamma_2\Gamma_1} \quad \text{.....(C-4)}$$

$$c_2 = \frac{\Gamma_1}{\Gamma_1 - \Gamma_2 e^{(\Gamma_2-\Gamma_1)} + \varepsilon_D \Gamma_2 \Gamma_1 e^{(\Gamma_2-\Gamma_1)} - \varepsilon_D \Gamma_2 \Gamma_1} \quad \text{.....(C-5)}$$

The outlet concentration is calculated by eqs. C-3, C-4 and C-5.

$$C(1) = \frac{(\Gamma_1 - \Gamma_2) e^{\Gamma_2}}{\Gamma_1 - \Gamma_2 e^{(\Gamma_2-\Gamma_1)} + \varepsilon_D \Gamma_2 \Gamma_1 \left(e^{(\Gamma_2-\Gamma_1)} - 1\right)} \quad \text{.....(C-6)}$$

It is worth mentioning that application of both inlet boundary conditions, eqs. B-3, B-4 and B-5, results in the same solution in the eq. B-10 for $V = V(x_D)$. So, the equation for barium concentration $C(x_D)$, eq. B-12, is the same for both cases. An application of inlet boundary conditions eq. B-5 also results in explicit solution that differs from eqs. C-3 to C-5. Nevertheless, the calculations show that the difference in distributions of $C(x_D)$ and $Y(x_D)$ for both types of inlet boundary conditions is negligibly small for the range of parameters ε_D and ε_k in oil reservoirs.

The equation for first order approximation is:

$$\varepsilon_D \frac{d^2 C_1}{dx_D^2} - \frac{dC_1}{dx_D} - \varepsilon_k C_1 - \varepsilon_k C_0^2 + \varepsilon_k C_0 = 0 \quad \text{.....(C-7)}$$

Substituting expansion eq. C-1 into boundary conditions, eqs. A-10 and B-3; and integrating the linear non-homogeneous eq. C-7, obtain first order approximation:

$$C_1(x_D) = c_3 e^{\Gamma_1 x_D} + c_4 e^{\Gamma_2 x_D} + K_1 e^{2\Gamma_1 x_D} + K_2 e^{(\Gamma_1+\Gamma_2)x_D} + K_3 e^{2\Gamma_2 x_D} + K_4 x_D e^{\Gamma_1 x_D} + K_5 x_D e^{\Gamma_2 x_D} \quad \text{.....(C-8)}$$

Here constants c_3 and c_4 are obtained from boundary conditions; constants $K_1, K_2 \ldots K_5$ are calculated during solution of inhomogeneous linear eq. C-7 where C_0 is a zero order approximation, eq. C-3.

The equation for second order approximation is also obtained by substitution of expansion eq. C-1 into eq. B-12:

$$\varepsilon_D \frac{d^2 C_2}{dx_D^2} - \frac{dC_2}{dx_D} - \varepsilon_k C_2 + 2\varepsilon_k C_1 - 4\varepsilon_k C_0 C_1 = 0 \quad \text{.....(C-9)}$$

The solution provides with second order approximation

$$C_2(x_D) = c_5 e^{\Gamma_1 x_D} + c_6 e^{\Gamma_2 x_D} + (m_0 + m_1 x_D) e^{2\Gamma_1 x_D} + (m_2 + m_3 x_D) e^{(\Gamma_1+\Gamma_2)x_D} + (m_4 + m_5 x_D) e^{2\Gamma_2 x_D} + (m_6 + m_7 x_D) x_D e^{\Gamma_1 x_D} + (m_8 + m_9 x_D) x_D e^{\Gamma_2 x_D} + n_1 e^{(2\Gamma_1+\Gamma_2)x_D} + n_2 e^{(\Gamma_1+2\Gamma_2)x_D} + n_3 e^{3\Gamma_1 x_D} + n_4 e^{3\Gamma_2 x_D} \quad \text{.....(C-10)}$$

Appendix D. Coreflood "Productivity Index"

Let us calculate the pressure drop in the core during flow with salt precipitation

$$\Delta p = -\int_0^L \frac{\partial p}{\partial x} dx = \frac{U\mu}{k_o} \int_0^L (1 + \beta\sigma)\, dx \quad \text{.....(D-1)}$$

Substituting dimensionless deposited concentration eq. A-6, we obtain

$$\Delta p = \frac{U\mu}{k_0} \left(1 + \beta c_{Ba}^0 \frac{M_{BaSO_4}}{\rho_{BaSO_4}} \int_0^1 S(x_D)\, dx_D\right) \quad \text{.....(D-2)}$$

The deposited concentration is calculated from system of equations A-7.

$$\int_0^1 S(x_D)\, dx_D = \varepsilon_k t_D \int_0^1 C(x_D) Y(x_D) dx_D \quad \text{.....(D-3)}$$

The final expression for the pressure drop on the core is:

$$\Delta p = \frac{U\mu}{k_0} \left(1 + \beta \varepsilon_k c_{Ba}^0 \frac{M_{BaSO_4}}{\rho_{BaSO_4}} t_D \int_0^1 C(x_D) Y(x_D)\, dx_D\right) \quad \text{...(D-4)}$$

Let us introduce the following dimensionless impedance function that is an inverse to dimensionless productivity index

$$J(t_D) = \frac{U^0}{\Delta p^0} \frac{\Delta p}{U} \quad \text{.....(D-5)}$$

The impedance expression follows from eqs. D-4 and D-5.

$$\frac{PI^0}{PI}=\left(1+\beta\varepsilon_k c_{Ba}^0\frac{M_{BaSO_4}}{\rho_{BaSO_4}}t_D\int_0^1 C(x_D)Y(x_D)dx_D\right)\ldots\ldots\text{(D-6)}$$

So, the impedance is a linear function of time

$$J(t_D)=1+mt_D$$

$$m=\frac{\beta\varepsilon_k c_{Ba}^0 M_{BaSO_4}}{\rho_{BaSO_4}}\int_0^1 C(x_D)Y(x_D)dx_D \quad\ldots\ldots\ldots\ldots\ldots\ldots\text{(D-7)}$$

Equation D-7 allows for determination of formation damage coefficient, β, from the pressure drop and flow rate data.

Figure Captions

Fig. 1—Precipitation of barium sulphate in the mixing zone
a) in stream tube during displacement of formation water by injection water;
b) in the reservoir.

Fig. 2—Experimental setup schema

Fig. 3—Photo of the core and schema of quasy-steady state test

Fig. 4—Diffusion coefficient vs. velocity for two cores
[Sample 1: ◊ (lnD = 1.0859 lnU-3.8995, R2 = 0.875)
Sample 2: □ (lnD = 0.8689 lnU-6.3264, R2 = 0.9933)]

Fig. 5—Barium Concentration profile for numerical and asymptotic approximation solution

Fig. 6—Function of the relative error between numerical solution and asymptotic expansions solution versus concentrations ration α

Fig. 7—Dependence of chemical rate coefficient versus flow velocity
a) test 1;
b) test 2

Fig. 8—Distribution function for parameter λ and β due all laboratorial tests
a) Kinetics coefficient λ $(M*m)^{-1}$
b) Formation damage coefficient β

Fig. 9—Barium Concentration profile versus seawater fraction in produced water for Well X1, Campos Basin

Fig. 10—Productivity index decline versus real time in days, for Well X1, Campos Basin

Fig. 11—Barium Concentration profile versus seawater fraction in produced water for Well X2, Campos Basin

Fig. 12—Distribution function for parameter λ and β due all field studies
a) Kinetics coefficient λ $(M*m)^{-1}$
b) Formation damage coefficient β

TABLE 1—KINETICS AND FORMATION DAMAGE COEFFICIENTS AS OBTAINED FROM COREFLOOD TESTS, AT TEMPERATURE 20°C, BY TODD, A. AND YUAN, M., (1989)

	α_D = 0.005 m		α_D = 0.01 m		α_D = 0.03 m	
Brine	λ, $(M*m)^{-1}$	β	λ, $(M*m)^{-1}$	β	λ, $(M*m)^{-1}$	β
BSS0	10740	79.06	12200	70.79	18585	48.18
BSS1	4974	98.50	5575	89.18	8268	62.01
BS2	239	63.35	263	58.07	371	41.82
BS2	410	14.50	454	13.25	658	9.39
BS3	1969	17.07	2266	14.45	3554	9.12

TABLE 2—KINETICS AND FORMATION DAMAGE COEFFICIENTS AS OBTAINED FROM COREFLOOD TESTS, AT TEMPERATURE 70°C, BY TODD, A. AND YUAN, M., 1989

	α_D = 0.005 m		α_D = 0.01 m		α_D = 0.03 m	
Brine	λ $(M*m)^{-1}$	β	λ $(M*m)^{-1}$	β	λ $(M*m)^{-1}$	β
BA	17450	37.71	20200	33.23	31850	21.92
BSS0	23720	78.90	26100	70.62	42200	45.62
BSS1	5540	42.98	6235	38.77	9310	26.81
BSS2	1533	73.25	1760	65.00	2760	43.05
Water 1	922	96.37	1043	86.65	1578	59.34

TABLE 3—COMPOSITIONS OF SIMPLE BRINES USED IN COREFLOOD TESTS, BY GOULDING P. S.,1987

Mixed Brine	Incompatible Waters	Ba^{2+}(M)	SO_4^{2+}(M)
D	Ba rich	0.0025	0.0
	SO_4 rich	0.0	0.0025
E	Ba rich	0.00125	0.0
	SO_4 rich	0.0	0.00125
F	Ba rich	0.0006	0.0
	SO_4 rich	0.0	0.0006
H	Ba rich	0.004	0.0
	SO_4 rich	0.0	0.004
I	Ba rich	0.004	0.0
	SO_4 rich	0.0	0.004
J	Ba rich	0.004	0.0
	SO_4 rich	0.0	0.004

TABLE 4—KINETICS AND FORMATION DAMAGE COEFFICIENTS AS OBTAINED FROM COREFLOODS, BY GOULDING P. S.,1987

	α_D = 0.005 m		α_D = 0.01 m		α_D = 0.03 m	
Brine	λ, $(M*m)^{-1}$	β	λ, $(M*m)^{-1}$	β	λ, $(M*m)^{-1}$	β
C221515DD	63390	1228.02	77300	1015.44	133590	607.16
C221515DD	80700	177.48	101250	143.13	183850	81.50
C167.57.5EE	68800	2954.54	79350	2565.81	123100	1695.45
C237.57.5FF	107780	246.63	122480	217.22	184450	147.32
C167.57.5FF	72260	164.50	81860	146.48	121560	101.13
C267.57.5HH	31900	60.89	38025	51.38	62950	32.01
C247.57.5II	45990	156.53	57075	127.48	101640	73.97
C247.57.5II	49440	78.10	61860	63.13	111840	36.09
C247.57.5JJ	51320	111.23	64200	98.46	115910	72.54
C247.57.5JJ	52900	52.06	66450	46.02	120740	33.71

TABLE 5—VALUES OF KINETICS AND FORMATION DAMAGE COEFFICIENTS AS OBTAINED FROM COREFLOODS

Coreflood Test	Kinetics Coefficient λ, $(M*m)^{-1}$	Formation Damage Coefficient β
Lopes Jr., 2002	3003 – 3951	-
Yuan et al., 1989		
BSS0 (20ºC)	10740 – 18585	48 – 79
BSS1 (20ºC)	4974 – 8268	62 – 98
BS2 (20ºC)	239 – 658	42 – 63
BS3 (20ºC)	1969 – 3554	9 – 17
BA (70ºC)	17450 – 31850	22 – 38
BSS0 (70ºC)	23720 – 42200	46 – 79
BSS1 (70ºC)	5540 – 9310	27 – 43
BSS2 (70ºC)	1553 – 2760	43 – 74
Water 1 (70ºC)	922 – 1578	60 – 97
Goulding P. S., 1987		
C221515DD-2S	63390 – 133590	607.16 – 1228.02
C221515DD-8S	80700 – 183850	81.50 – 177.48
C167.57.5EE-11S	68800 – 123100	1695.45 – 2954.54
C237.57.5FF-1S	107780 – 184450	147.32 – 246.63
C167.57.5FF-2S	72260 – 121560	101.13 – 164.50
C267.57.5HH-1S	31900 – 62950	32.01 – 60.89
C247.57.5II-1S	45990 – 101640	73.97 – 156.53
C247.57.5II-2S	49440 – 111840	36.09 – 78.10
C247.57.5JJ-1S	51320 – 115910	72.52 – 111.23
C247.57.5JJ-2S	52900 – 120740	33.71 – 52.06
Wat et al., 1992	798 – 963	-

TABLE 6—KINETICS COEFFICIENT VALUES BASED ON WELLS DATA FROM FIELD X

Field Information				α_D = 0.005 m	α_D = 0.01 m	α_D = 0.03 m
Field X	c_{Ba}^0, ppm	c_{SO4}^0, ppm	R_c, m	λ, $(M*m)^{-1}$	λ, $(M*m)^{-1}$	λ, $(M*m)^{-1}$
Well X1	46	2990	0.127	5174	117234	409126
Well X2	46	2990	0.127	205	4039	30112

TABLE 7—VALUES OF KINETICS AND FORMATION DAMAGE COEFFICIENTS AS OBTAINED FROM FIELD DATA

Field Data	Kinetics Coefficient λ, $(M*m)^{-1}$	Formation Damage Coefficient β
Field X (Campos Basin)		
Well X1	5000 – 120000	0.5 – 2
Well X2	200 – 3000	
Field N (Campos Basin)		
Well NA-16	10 – 210	35 – 565
Well NA-37	7 – 150	100 – 1800
Well NA-52	50 – 1000	700 – 2000
North Sea		
Field A	100 – 900	–
Field B	2 – 750	–
Field C	300 – 3000	–
Field D	60 – 600	–
Field E	100 – 1000	–

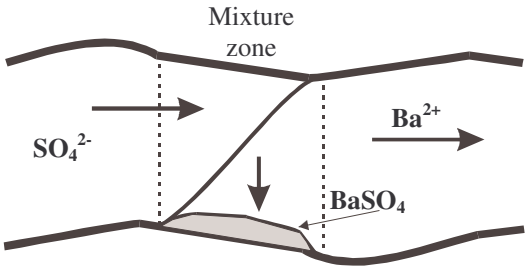

1a)

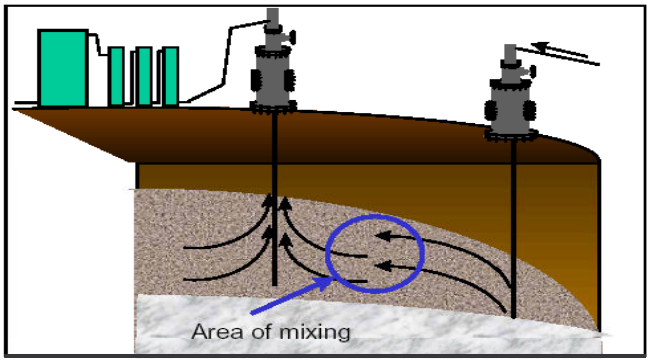

1b)

Fig. 1—Precipitation of barium sulphate in the mixing zone
a) in stream tube during displacement of formation water by injection water;
b) in the reservoir.

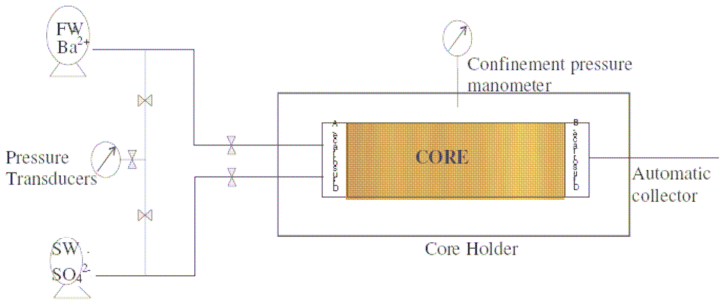

Fig 2—Experimental setup schema

Fig. 3—Photo of the core and schematic of quasy steady state test

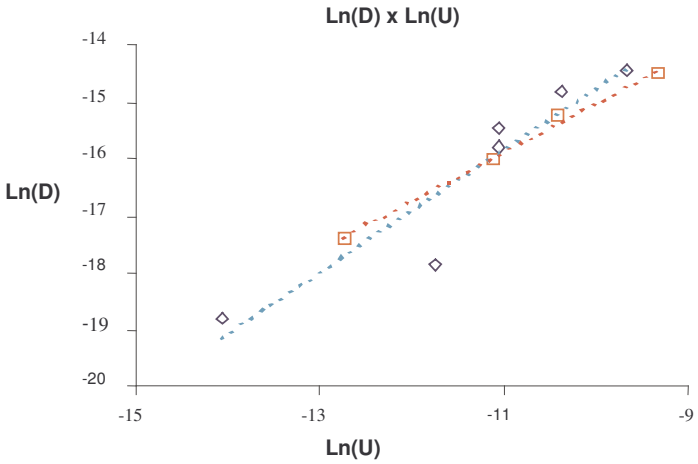

Fig. 4—Diffusion coefficient vs. velocity for two cores [Sample 1: ◊ (lnD = 1.0859 lnU–3.8995, R2 = 0.875) Sample 2: □ (lnD = 0.8689 lnU–6.3264, R2 = 0.9933)]

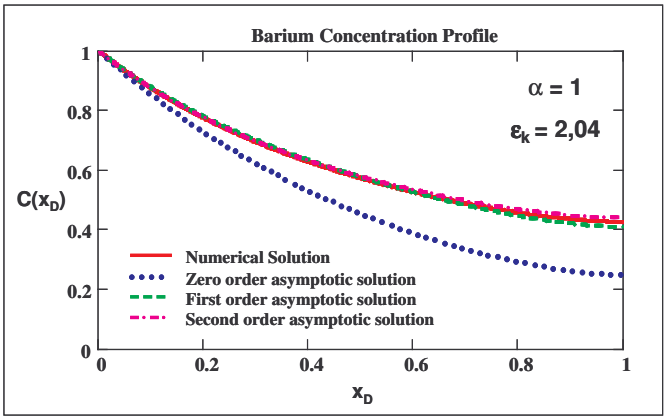

Fig. 5—Barium Concentration profile for numerical and asymptotic approximation solution

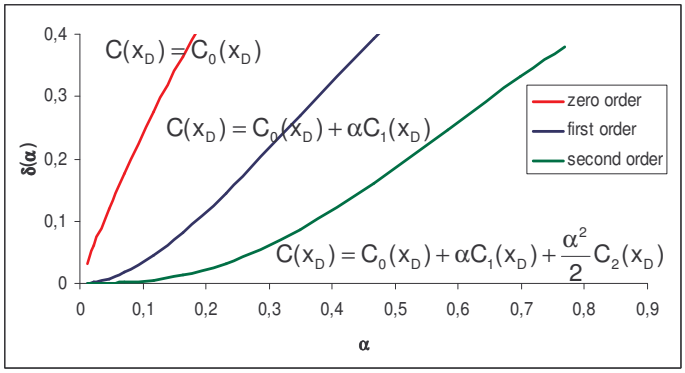

Fig. 6—Function of the relative error between numerical solution and asymptotic expansions solution versus concentrations ration α.

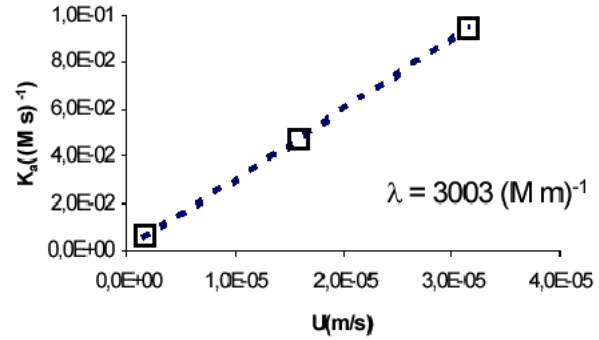

7a)

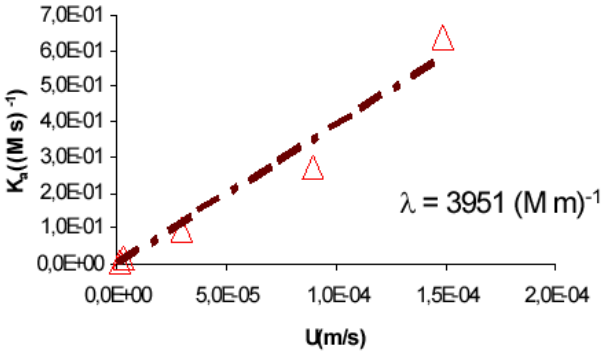

7b)

Fig. 7—Dependence of chemical rate coefficient versus flow velocity
a) test 1; b) test 2

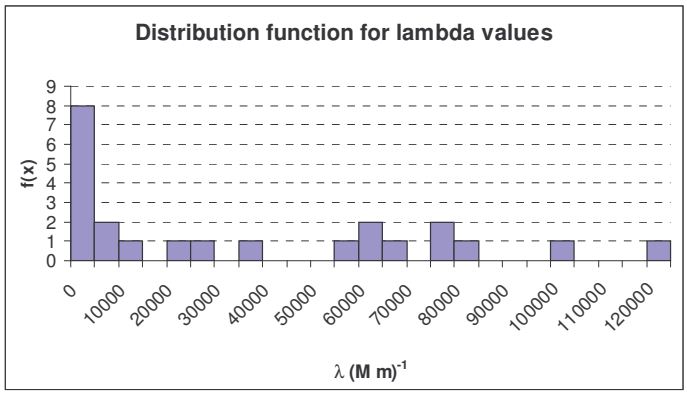

8a)

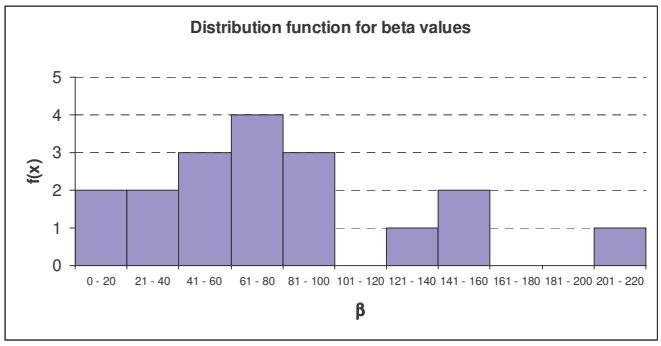

8b)

Fig. 8—Distribution function for parameter λ and β due all laboratorial tests
a) Kinetics coefficient λ $(M*m)^{-1}$
b) Formation damage coefficient β

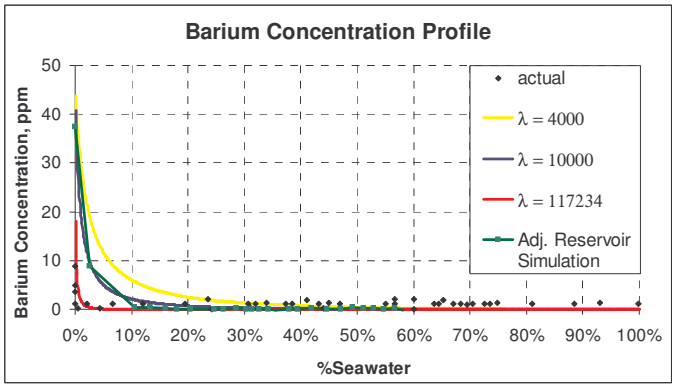

Fig. 9—Barium Concentration profile versus seawater fraction in produced water for Well X1, Campos Basin.

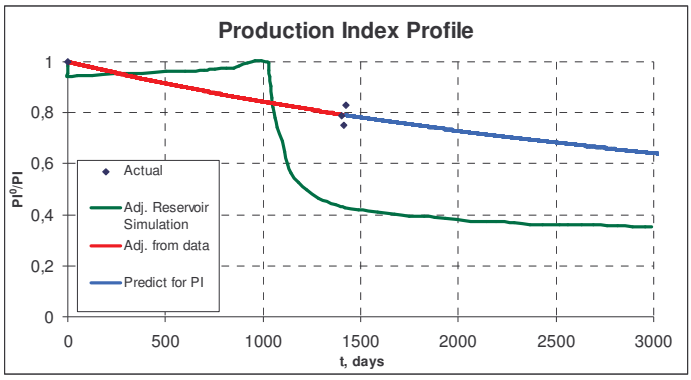

Fig. 10—Productivity index decline versus real time in days, for Well X1, Campos Basin.

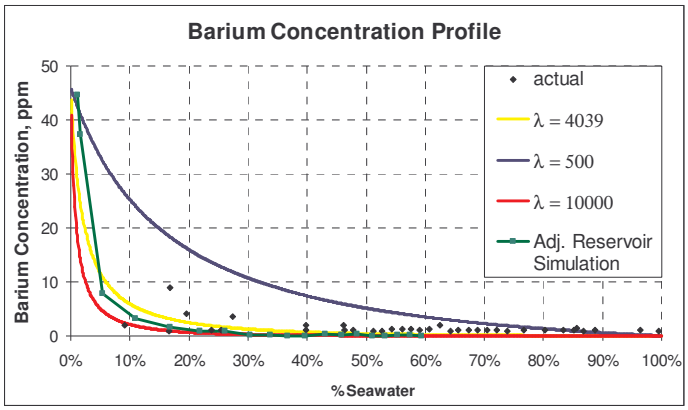

Fig. 11—Barium Concentration profile versus seawater fraction in produced water for Well X2, Campos Basin.

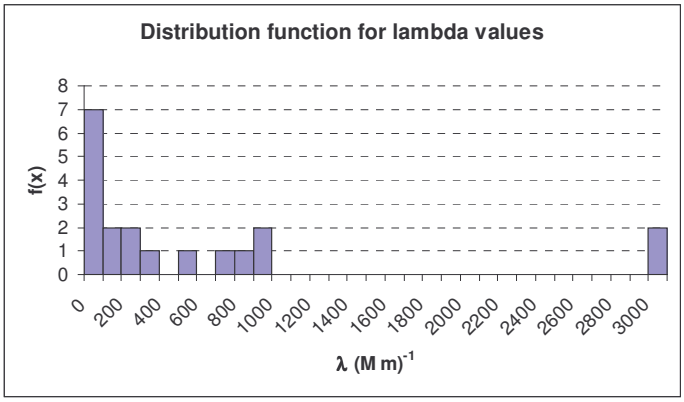

12a)

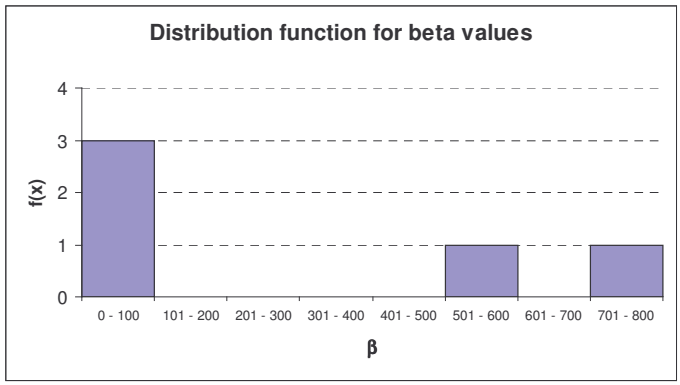

12b)

Fig. 12—Distribution function for parameter λ and β due all field studies
a) Kinetics coefficient λ (M∗m)-1
b) Formation damage coefficient β